ANTIOXIDANTS & REDOX SIGNALING
Volume 20, Number 2, 2014

DOI: 10.1089/ars.2012.4918

Therapeutics

FORUM ORIGINAL RESEARCH COMMUNICATION

Nox2-Induced Production of Mitochondrial Superoxide in Angiotensin II-Mediated Endothelial Oxidative Stress and Hypertension

Sergey I. Dikalov,[1] Rafal R. Nazarewicz,[1] Alfiya Bikineyeva,[1] Lula Hilenski,[2] Bernard Lassègue,[2] Kathy K. Griendling,[2] David G. Harrison,[1] and Anna E. Dikalova[1]

Abstract

Aims: Angiotensin II (AngII)-induced superoxide ($O_2^{\bullet -}$) production by the NADPH oxidases and mitochondria has been implicated in the pathogenesis of endothelial dysfunction and hypertension. In this work, we investigated the specific molecular mechanisms responsible for the stimulation of mitochondrial $O_2^{\bullet -}$ and its downstream targets using cultured human aortic endothelial cells and a mouse model of AngII-induced hypertension. ***Results:*** Western blot analysis showed that Nox2 and Nox4 were present in the cytoplasm but not in the mitochondria. Depletion of Nox2, but not Nox1, Nox4, or Nox5, using siRNA inhibits AngII-induced $O_2^{\bullet -}$ production in both mitochondria and cytoplasm. Nox2 depletion in gp91phox knockout mice inhibited AngII-induced cellular and mitochondrial $O_2^{\bullet -}$ and attenuated hypertension. Inhibition of mitochondrial reverse electron transfer with malonate, malate, or rotenone attenuated AngII-induced cytoplasmic and mitochondrial $O_2^{\bullet -}$ production. Inhibition of the mitochondrial ATP-sensitive potassium channel ($mitoK^+_{ATP}$) with 5-hydroxydecanoic acid or specific PKCε peptide antagonist (EAVSLKPT) reduced AngII-induced H_2O_2 in isolated mitochondria and diminished cytoplasmic $O_2^{\bullet -}$. The $mitoK^+_{ATP}$ agonist diazoxide increased mitochondrial $O_2^{\bullet -}$, cytoplasmic c-Src phosphorylation and cytoplasmic $O_2^{\bullet -}$ suggesting feed-forward regulation of cellular $O_2^{\bullet -}$ by mitochondrial reactive oxygen species (ROS). Treatment of AngII-infused mice with malate reduced blood pressure and enhanced the antihypertensive effect of mitoTEMPO. Mitochondria-targeted H_2O_2 scavenger mitoEbselen attenuated redox-dependent c-Src and inhibited AngII-induced cellular $O_2^{\bullet -}$, diminished aortic H_2O_2, and reduced blood pressure in hypertensive mice. ***Innovation and Conclusions*:** These studies show that Nox2 stimulates mitochondrial ROS by activating reverse electron transfer and both mitochondrial $O_2^{\bullet -}$ and reverse electron transfer may represent new pharmacological targets for the treatment of hypertension. *Antioxid. Redox Signal.* 20, 281–294.

Introduction

HYPERTENSION AFFECTS MORE THAN 50 million individuals in the United States and represents a serious health challenge for Western societies (10); however, many patients' blood pressure remains poorly controlled despite treatment with multiple drugs. Endothelial dysfunction plays a key role in the development of this disease and is associated with decreased bioavailability of nitric oxide ($NO^{\bullet}$) and overproduction of vascular reactive oxygen species (ROS), such as $O_2^{\bullet -}$ and H_2O_2 (25). While the role of angiotensin II (AngII) in hypertension has been known for decades, it has been recently found that this octapeptide promotes the production of vascular ROS both in the cellular cytoplasm and in the mitochondria (17). We have previously shown that mitochondria-targeted antioxidants may represent a new class of antihypertensive agents (17). The exact molecular mechanisms of AngII-induced production of mitochondrial ROS are not well defined. It has been shown that depletion of the $p22^{phox}$ subunit of NADPH oxidase with siRNA inhibits mitochondrial ROS

[1]Division of Clinical Pharmacology, Vanderbilt University Medical Center, Nashville, Tennessee.
[2]Division of Cardiology, Emory University School of Medicine, Atlanta, Georgia.

Innovation

It has been recently shown that mitochondrial $O_2^{\bullet -}$ contributes to endothelial dysfunction and hypertension; however, the exact mechanisms and the targets of mitochondrial reactive oxygen species (ROS) have not been identified. In this work, we have investigated the specific molecular mechanisms responsible for the stimulation of mitochondrial $O_2^{\bullet -}$ and its downstream targets. First, we have identified cytoplasmic Nox2 isoform of NADPH oxidase as an activator of mitochondrial ROS. Second, for the first time, we have shown redox-sensitive upregulation of reverse electron transport as a major source of mitochondrial ROS. Third, the target of mitochondrial ROS is a cytoplasmic c-Src, which maintains the Nox2 activity, and inhibition of mitochondrial ROS attenuates c-Src and Nox2 activity. Finally, our *in vivo* experiments have demonstrated that both mitochondrial ROS and reverse electron transfer may represent new pharmacological targets for the treatment of hypertension.

production in response to AngII, and inhibition of NADPH oxidase improves mitochondrial function (20). Furthermore, the production of AngII-induced ROS was attenuated by the inhibition of mitochondrial ATP-sensitive potassium channels (mitoK^+_{ATP}) with 5-hydroxydecanoic acid (5HD) (20). These data suggest that AngII could induce the production of mitochondrial ROS by the activation of NADPH oxidases and the stimulation of redox-sensitive mitoK^+_{ATP} (43).

NADPH oxidases are a family of enzyme complexes that catalyze the transfer of electrons from NADPH to molecular oxygen *via* their "Nox" catalytic subunit, generating $O_2^{\bullet -}$ and H_2O_2. The Nox proteins vary in terms of their mode of activation, localization, and physiological functions (34). Human endothelial cells express four Nox isoforms: Nox1, Nox2, Nox4, and Nox5 (1, 27). AngII is the major effector hormone of the renin–angiotensin system and plays an important role in the activation of vascular NADPH oxidases through PKC- and c-Src-dependent pathways (36). Initial activation of the angiotensin II receptor (AT1R) leads to PKC-mediated phosphorylation of $p47^{phox}$. This leads to c-Src activation and stimulation of the epidermal growth factor receptor, which evokes phosphatidylinositol 3-kinase-dependent production of phosphatidylinositol (3,4,5)-trisphosphate, activating the Rac1 subunit of NADPH oxidase, at least in vascular smooth muscle cells (45). Nox4 and Nox5 do not require $p47^{phox}$ or Rac1 subunits (39). Thus, in vascular cells, AngII primarily increases the activity of Nox1 or Nox2 (35). Activation of c-Src is redox sensitive and is stimulated by H_2O_2 (50) and thus may provide a feed-forward stimulation of ROS production. It has been reported that both Nox1 and Nox2 contribute to the development of hypertension (5, 18); however, the Nox isoform responsible for the stimulation of mitochondrial ROS in endothelial cells has not been identified.

It has been recently reported that the activation of mitochondrial ATP-sensitive potassium channels (mitoK_{ATP}) increases the production of mitochondrial ROS (3, 20), and this process is dependent on the activity of PKCε. PKCε is exquisitely redox sensitive and therefore is a very good candidate to transduce signals from extramitochondrial ROS leading to mitochondrial ROS production (11). Although it has been suggested that mitoK_{ATP} can stimulate mitochondrial $O_2^{\bullet -}$ production by complex I (3), the exact mechanisms and site of mitochondrial ROS release are not well understood.

In this work, we investigated the role of specific Nox isoforms in the regulation of mitochondrial ROS by AngII and evaluated the potential role of mitoK_{ATP} and reverse electron transfer in the production of AngII-induced mitochondrial ROS.

Results

Attenuation of AngII-induced $O_2^{\bullet -}$ by depletion of Nox2

We have previously shown that the depletion of the $p22^{phox}$ docking subunit of NADPH oxidases attenuates AngII-induced production of mitochondrial ROS (20). We therefore investigated the role of specific NADPH oxidase isoforms using siRNA. Cultured HAEC were transfected with siNox1, siNox2, siNox4, siNox5, or nonsilencing siRNA (NS siRNA) 72 h before the experiments. These conditions have been previously shown to significantly diminish the expression of Nox subunits (15, 26) (Supplementary Fig. S1; Supplementary Data are available online at www.liebertpub.com/ars). Intact HAEC were treated with saline or AngII for 4 h before measurements of cytoplasmic or mitochondrial $O_2^{\bullet -}$ using dihydroethidium (DHE) or dihydroethidium conjugate with hexyl triphenylphosphonium (MitoSOX) (Fig. 1). As evident in Figure 1A, transfection with siNox1, siNox4, and siNox5 did not abolish AngII-mediated stimulation of cytoplasmic $O_2^{\bullet -}$ measured by confocal fluorescence microscopy and DHE probe. Only siNox2 completely abrogated AngII-stimulated production of cytoplasmic $O_2^{\bullet -}$. These data indicate that Nox2 is the primary source of AngII-induced cytoplasmic $O_2^{\bullet -}$ in endothelial cells. Analysis of mitochondrial $O_2^{\bullet -}$ using the specific probe MitoSOX showed that transfection with siNox1, siNox4, or siNox5 inhibits AngII-induced production of mitochondrial $O_2^{\bullet -}$; however, the depletion of Nox2 completely abolished AngII-mediated increase of mitochondrial $O_2^{\bullet -}$ (Fig. 1B). It has been previously shown that $O_2^{\bullet -}$ measurements by DHE and MitoSOX can be affected by the formation of nonspecific fluorescent products (14). We therefore confirmed $O_2^{\bullet -}$ measurements by DHE and MitoSOX using HPLC analysis (Fig. 1C). Stimulation of NS siRNA-treated HAEC with AngII (200 n*M*, 4 h) significantly increased the accumulation of $O_2^{\bullet -}$ specific product of DHE (2-OH-E^+) and MitoSOX (2-OH-Mito-E^+) confirming the stimulation of cytoplasmic and mitochondrial $O_2^{\bullet -}$ by AngII. Transfection with siNox5 did not affect $O_2^{\bullet -}$ production. Transfection with siNox2, however, significantly inhibited AngII-induced $O_2^{\bullet -}$ production both in the cytoplasm and in the mitochondria (Fig. 1C). These HPLC data, therefore, provided validation of $O_2^{\bullet -}$-specific measurements using confocal microscopy and confirmed a key role of Nox2 in AngII-mediated $O_2^{\bullet -}$ production.

Analysis of cellular and mitochondrial localization of Nox isoforms

It has been recently suggested that NADPH oxidases within mitochondria may be a source of mitochondrial $O_2^{\bullet -}$ (2). We therefore examined the presence of Nox isoforms in the whole cell lysate and in mitochondrial fractions. Western blots showed the significant presence of Nox1, Nox2, and

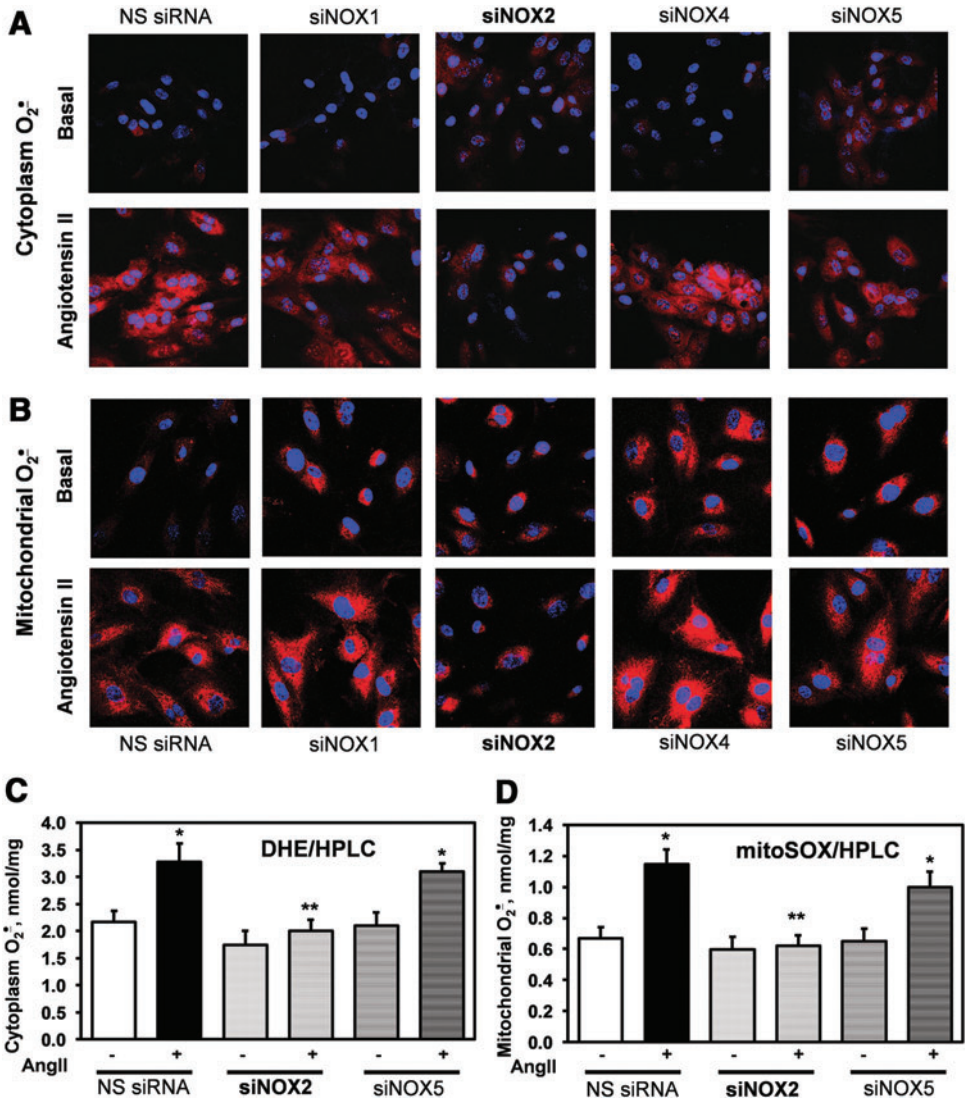

FIG. 1. Attenuation of AngII-induced cytoplasmic and mitochondrial $O_2^{\bullet-}$ by depletion of Nox2 using siRNA. (A) Effect of Nox isoform depletion on cytoplasmic $O_2^{\bullet-}$ production measured by DHE and confocal microscopy. **(B)** Effect of Nox depletion on mitochondrial $O_2^{\bullet-}$ production measured by MitoSOX and confocal microscopy. Effect of Nox2 and Nox5 depletion on cytoplasmic and mitochondrial $O_2^{\bullet-}$ measured by HPLC analysis of DHE-treated **(C)** and MitoSOX-treated **(D)** samples. HAEC were treated with siRNAs for 72 h and then incubated with saline (basal) or stimulated with 200 n*M* AngII for 4 h before application of DHE or MitoSOX probes. Panels **(A, B)** show typical images from confocal microscopy studies with siRNA-transfected HAEC obtained in three independent experiments. $^{*}p < 0.01$ *versus* NS siRNA, $^{**}p < 0.05$ *versus* AngII. AngII, angiotensin II; DHE, dihydroethidium; HAEC, human aortic endothelial cells; MitoSOX, dihydroethidium conjugate with hexyl triphenylphosphonium; NS siRNA, nonsilencing siRNA. To see this illustration in color, the reader is referred to the web version of this article at www.liebertpub.com/ars

Nox4 in cellular lysates of HAEC (Fig. 2); however, no Nox catalytic subunits were present in mitochondrial samples. These data are in agreement with previously reported localization of Nox subunits in the cytoplasm and nucleus but not in the mitochondria (13, 27). A preliminary analysis of vascular and kidney tissue did not show Nox isoforms in isolated mitochondria but revealed Nox presence in cytoplasmic fractions (data not shown).

Inhibition of AngII-induced $O_2^{\bullet-}$ and hypertension in Nox2 knockout mice

To test *in vivo* pathophysiological role of Nox2 in AngII-induced mitochondrial $O_2^{\bullet-}$ and hypertension, we have used Nox2 knockout mice (gp91phox KO) (22). Nox2KO and wild-type littermates (C57Bl/6J) were infused for 10 days with saline (vehicle) or AngII (0.7 mg/kg/day). Analysis of systolic blood pressure showed significant attenuation of hypertension in AngII-infused Nox2KO mice compared with wild-type littermates (Fig. 3A). Following AngII infusion, mice were sacrificed and aortic vessels were isolated for the analysis of cytoplasmic and mitochondrial $O_2^{\bullet-}$ using DHE and MitoSOX. It was found that AngII infusion in wild-type mice significantly increased cytoplasmic and mitochondrial $O_2^{\bullet-}$ in aorta (Fig. 3B, C). Meanwhile, Nox2 depletion in Nox2KO mice completely abrogated AngII-induced $O_2^{\bullet-}$ production in aorta both in cytoplasm and in mitochondria (Fig. 3B, C). These data support Nox2 as a major source of vascular $O_2^{\bullet-}$ (33) and demonstrate the key role of Nox2 in AngII-induced vascular mitochondrial $O_2^{\bullet-}$ and hypertension (Fig. 3, Scheme).

Role of reverse electron transfer in AngII-induced $O_2^{\bullet-}$

We previously reported that reverse electron transport (RET) plays an important role in the production of mitochondrial ROS (42). We therefore sought to determine if RET would contribute to AngII-induced mitochondrial $O_2^{\bullet-}$. To monitor mitochondrial $O_2^{\bullet-}$ levels in intact cells, we used the mitochondria-specific fluorescent probe MitoSOX. Acute treatment with the Nox2-specific peptide inhibitor gp91ds abolished MitoSOX fluorescence signal in AngII-stimulated HAEC. Supplementation with the complex II inhibitor malonate or an inhibitor of RET, rotenone (44), significantly

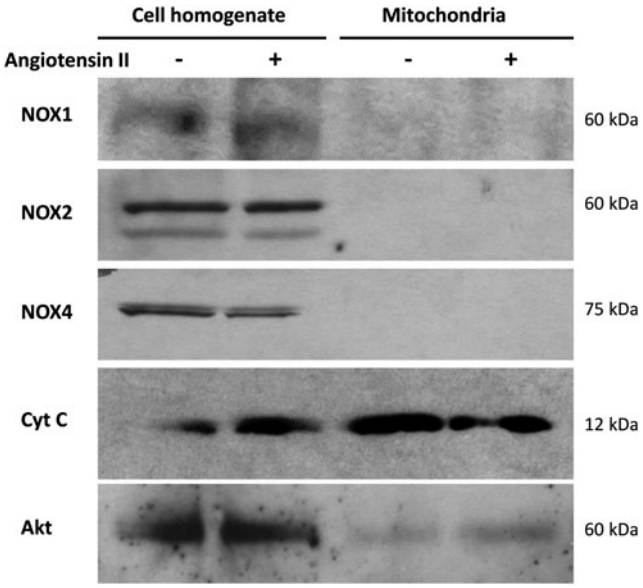

FIG. 2. Western blot analysis of cellular and mitochondrial Nox isoforms in HAEC. Cytochrome c (Cyt C) and serine-threonine kinase Akt were used as mitochondrial and cytoplasmic markers. Endothelial mitochondria do not contain Nox1, Nox2, and Nox4 isoforms. Figure shows representative Western blot of Nox1, Nox2, and Nox4 in HAEC homogenate and mitochondrial fractions obtained in three independent experiments.

decreased mitochondrial $O_2^{\bullet -}$ as reflected by MitoSOX fluorescence (Fig. 4A). Interestingly, as in the case of gp91ds, treatment with malonate or rotenone completely abolished cytoplasmic $O_2^{\bullet -}$ production in AngII-stimulated HAEC (Fig. 4B). The specificity of cytoplasmic $O_2^{\bullet -}$ measurements in these samples was confirmed by HPLC experiments where malate, malonate, and rotenone did not affect basal $O_2^{\bullet -}$ production but inhibited AngII-induced production of cytoplasmic $O_2^{\bullet -}$. As we have previously described, mitochondria-targeted superoxide dismutase (SOD) mimetic mitoTEMPO also inhibited cytoplasmic $O_2^{\bullet -}$ (Fig. 5) (17). It has been suggested that redox-sensitive PKCε can regulate the production of mitochondrial $O_2^{\bullet -}$ (11). Indeed, supplementation with the PKCε peptide antagonist EAVSLKPT inhibited mitochondrial $O_2^{\bullet -}$ production. Interestingly, the inhibition of PKCε also attenuated $O_2^{\bullet -}$ production in the cytoplasm (Fig. 4B).

Antihypertensive effect of malate and mitoTEMPO

The above studies show that reverse electron transfer plays an important role in AngII-induced production of both mitochondrial and cytoplasmic ROS. These data also suggest that reverse electron transfer can be potential pharmacological target for the treatment of hypertension. It has been previously reported that malate attenuates reverse electron transfer and inhibits the production of mitochondrial ROS both *in vitro* and *in vivo* (30, 42). We therefore performed additional studies *in vivo* infusing malate and mitoTEMPO after the onset of AngII-induced hypertension. Following 6 days of AngII infusion (0.7 mg/kg/day), systolic blood pressure reached 160 mm Hg (Fig. 6A). Subsequent treatment with malate resulted in a time-dependent decrease in blood pressure. As we have previously reported, mitoTEMPO treatment of hypertensive mice also decreased blood pressure (17). Interestingly, the combination of malate with mitoTEMPO was even more effective than either one alone (Fig. 6A). The role of Nox2 on mitochondrial $O_2^{\bullet -}$ in aortic tissue of hypertensive mice was confirmed by *ex vivo* treatment of aorta with Nox2-specific peptide inhibitor gp91ds-tat and measurements of mitochondrial $O_2^{\bullet -}$ by MitoSOX and HPLC. It was found that gp91ds-tat treatment of aorta isolated from hypertensive mice inhibited the production of mitochondrial $O_2^{\bullet -}$ to the level of

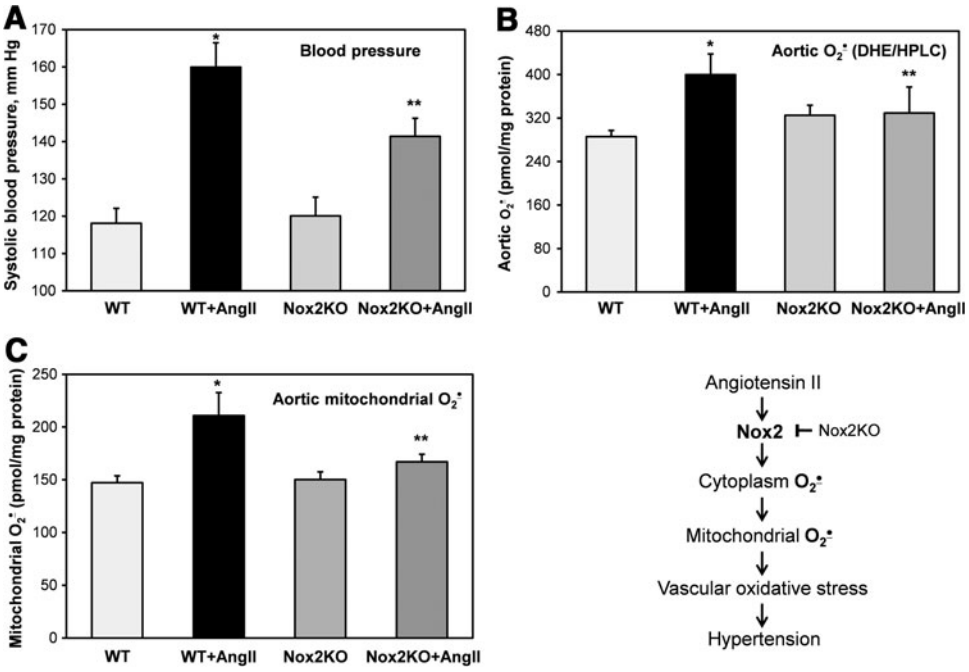

FIG. 3. Inhibition of AngII-induced hypertension and vascular $O_2^{\bullet -}$ production in gp91phox knockout mice (Nox2KO). (A) Blood pressure of wild-type (WT) C57Bl/6J and gp91phoxKO mice infused for 10 days with saline or AngII (0.7 mg/kg/day). **(B)** Measurements of cytoplasmic $O_2^{\bullet -}$ (DHE/HPLC) in aortas isolated from saline or AngII-infused mice. **(C)** Measurements of mitochondrial $O_2^{\bullet -}$ (MitoSOX/HPLC) in aortas isolated from saline or AngII-infused mice. Results represent mean ± SEM for five to eight animals per group. $^*p < 0.01$ *versus* control, $^{**}p < 0.05$ *versus* AngII.

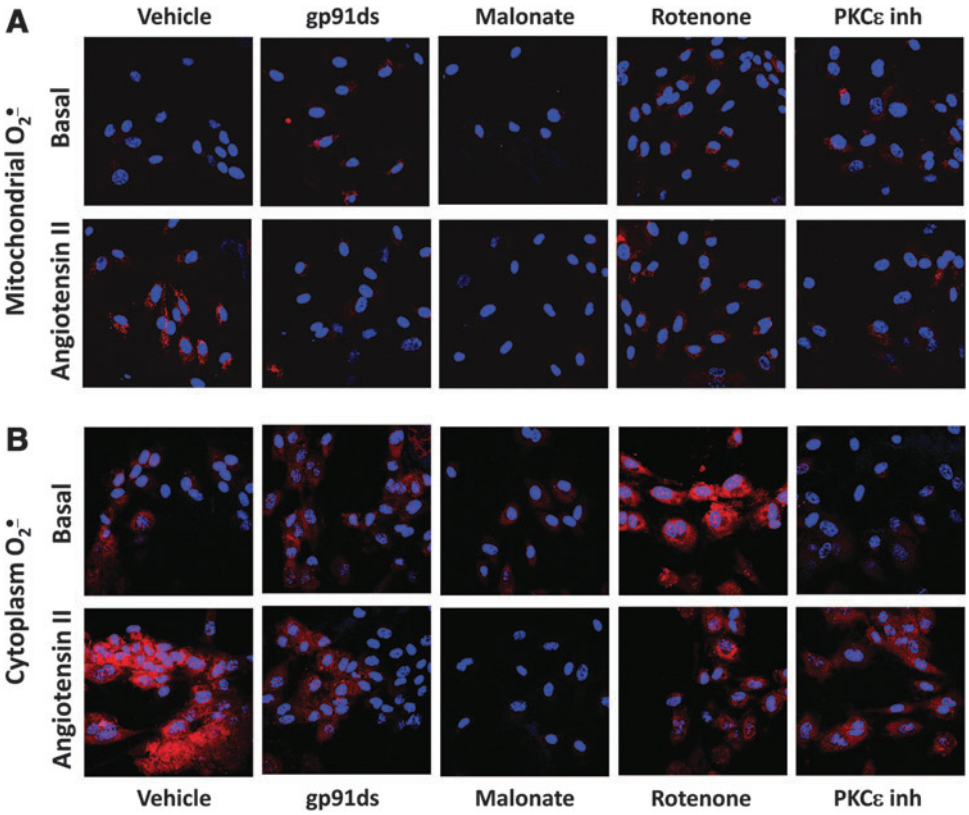

FIG. 4. Attenuation of mitochondrial and cytoplasmic $O_2^{\bullet-}$ by inhibition of reverse electron transfer with rotenone, malonate, or PKCε peptide antagonist. (A) Measurements of mitochondrial $O_2^{\bullet-}$ by MitoSOX and confocal microscopy. **(B)** Measurements of cytoplasmic $O_2^{\bullet-}$ by DHE and confocal microscopy. HAEC were incubated with saline (Basal) or stimulated with 200 n*M* AngII for 4 h and then treated with rotenone, malonate, or PKCε peptide antagonist EAVSLKPT before application of DHE or MitoSOX probes. Figure show typical images from confocal microscopy studies obtained in five independent experiments. To see this illustration in color, the reader is referred to the web version of this article at www.liebertpub.com/ars

normotensive animals (Fig. 6B). Interestingly, the inhibition of mitochondrial $O_2^{\bullet-}$ by malate or scavenging of mitochondrial $O_2^{\bullet-}$ by mitoTEMPO had additive effect on the reduction of aortic $O_2^{\bullet-}$ measured by DHE and HPLC (Fig. 6C). These data support the key role of Nox2 in the upregulation of mitochondrial $O_2^{\bullet-}$ by the reverse electron transfer and the presence of feed-forward interplay between mitochondrial and NADPH oxidase-derived $O_2^{\bullet-}$ in endothelial oxidative stress (Fig. 6, Scheme).

Feed-forward regulation of cellular $O_2^{\bullet-}$ by mitochondrial H_2O_2

These data demonstrate an important role of RET in AngII-induced production of mitochondrial $O_2^{\bullet-}$. Our data suggest the regulation of mitochondrial $O_2^{\bullet-}$ by PKCε; however, PKCε is expressed both in the cytoplasm and in the mitochondria. To further investigate the role of mitochondrial PKCε in AngII-mediated regulation of mitochondrial $O_2^{\bullet-}$, we analyzed the effect of PKCε peptide inhibitor on succinate-driven H_2O_2 production by mitochondria isolated from control and AngII-stimulated HAEC. The PKCε peptide antagonist EAVSLKPT significantly inhibited H_2O_2 production by mitochondria isolated from AngII-stimulated cells but did not affect H_2O_2 production by mitochondria isolated from unstimulated cells (Fig. 7A). The role of PKCε in the regulation of mitochondrial ROS potentially implicates mitoK_{ATP}, which is activated by PKCε (11). Indeed, treatment of isolated mitochondria with mitoK_{ATP} inhibitor 5HD significantly reduced H_2O_2 production (Fig. 7A).

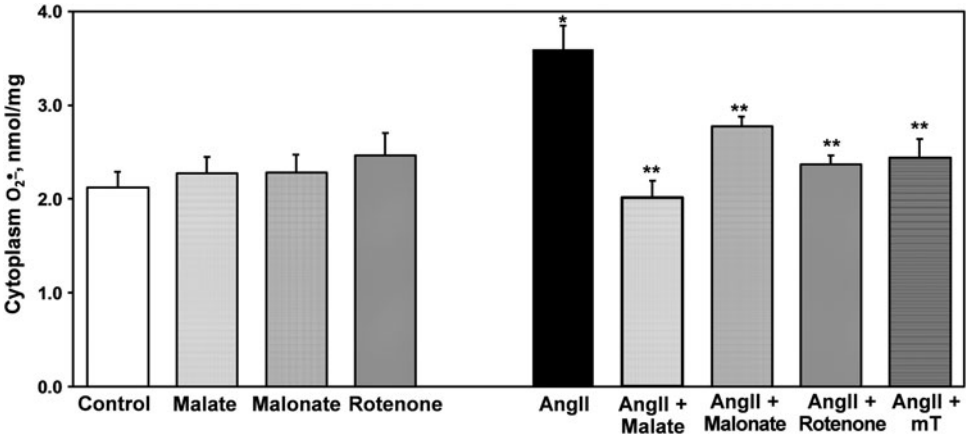

FIG. 5. Measurements of cytoplasmic $O_2^{\bullet-}$ in intact HAEC using DHE (10 μ*M*) and HPLC. Cells were treated with 200 n*M* AngII or saline as a vehicle and then supplemented with malate (0.1 m*M*), malonate (0.1 m*M*), rotenone (1 μ*M*), or mitoTEMPO (25 n*M*) for 15 min before application of DHE. *$p < 0.01$ *versus* controls, **$p < 0.05$ *versus* AngII ($n = 5$).

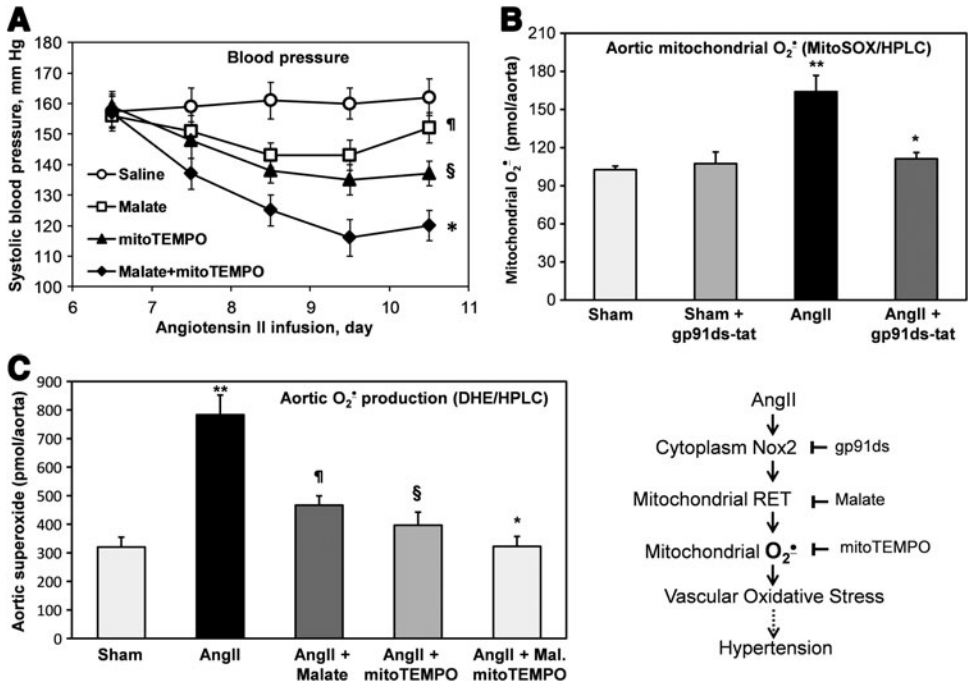

FIG. 6. Effects of malate or mitoTEMPO treatment after the onset of AngII-induced hypertension on blood pressure (A), aortic mitochondrial superoxide (B), and aortic cytoplasm superoxide (C). Systolic blood pressure in mice infused with saline, malate, mitoTEMPO (0.5 mg/kg/day), or malate plus mitoTEMPO after the onset of AngII-induced hypertension. Following 12 days of infusion, mice were sacrificed and aortas were isolated for superoxide analysis. Results represent mean ± SEM for six to eight animals per group. ¶$p < 0.05$ *versus* saline, §$p < 0.01$ *versus* saline, *$p < 0.05$ *versus* mitoTEMPO, **$p < 0.001$ *versus* sham.

These data demonstrate a role of PKCε and mitoK$_{ATP}$ in AngII-induced production of mitochondrial H_2O_2. The diminished release of mitochondrial H_2O_2 in cells treated with malonate, rotenone, or the PKCε peptide antagonist could explain reduced activity of the cytoplasmic NADPH oxidases and consequent decrease in cytoplasmic $O_2^{\bullet-}$ production (Fig. 4B) due to the attenuation of redox-dependent Nox2. We directly tested if scavenging of cytoplasmic H_2O_2 with PEG-catalase inhibits the production of cytoplasmic $O_2^{\bullet-}$ measured by conversion of DHE to the $O_2^{\bullet-}$-specific product 2-hydroxyethidium using HPLC. Supplementation of HAEC with cell-permeable H_2O_2 scavenger PEG-catalase (4) inhibited the production of cytoplasmic $O_2^{\bullet-}$ in AngII-stimulated cells but not affected $O_2^{\bullet-}$ production in control cells (Fig. 7B). We hypothesized that Nox2-derived H_2O_2 can diffuse to mitochondria and activate redox-dependent PKCε. Indeed, treatment with the PKCε peptide antagonist also inhibited AngII-stimulated cytoplasmic $O_2^{\bullet-}$ similar to PEG-catalase. These HPLC data demonstrate a potential feed-forward regulation of cytoplasmic $O_2^{\bullet-}$ by mitochondrial ROS. We have further investigated this process by treatment with mitoK$_{ATP}$ opener diazoxide (23), which is known to stimulate the production of mitochondrial ROS (3).

Effect of mitochondrial ROS on c-Src activity and endothelial oxidative stress

The studies described above indicate that AngII increases mitochondrial ROS production *via* PKCε activation and opening of mitoK$_{ATP}$. We investigated if the mitoK$_{ATP}$ agonist diazoxide mimics the AngII-mediated activation of mitoK$_{ATP}$ and could induce mitochondrial ROS and stimulate $O_2^{\bullet-}$ production in the cytoplasm. Supplementation of diazoxide increased mitochondrial $O_2^{\bullet-}$ as evident by an increase of

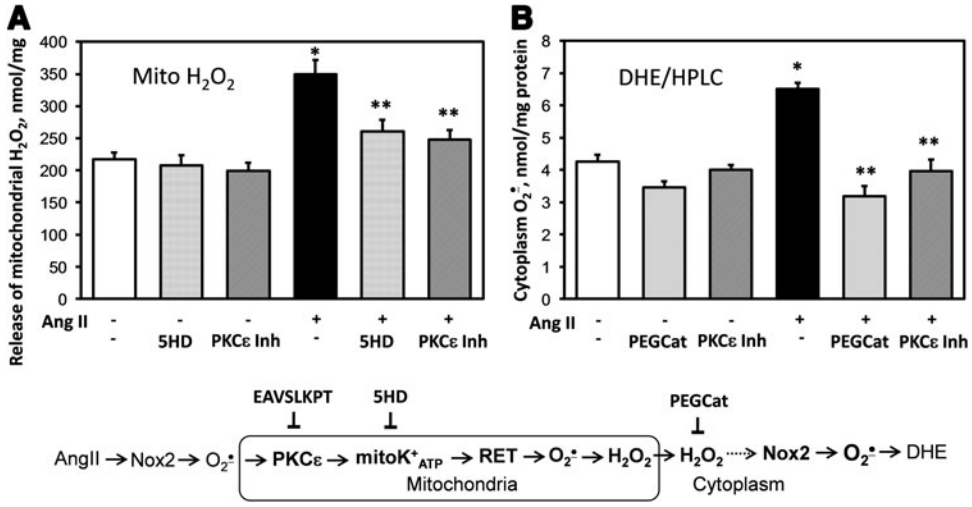

FIG. 7. Inhibition of PKCε reduces mitochondrial H_2O_2 (A) and cytoplasmic $O_2^{\bullet-}$ (B). **(A)** H_2O_2 was measured in isolated mitochondria supplemented with 10 m*M* succinate in the presence of saline, PKCε inhibitor EAVSLKPT (1 μ*M*), or 5HD (10 μ*M*) using ESR (17). **(B)** HPLC measurements of cellular $O_2^{\bullet-}$ in intact HAEC treated with 100 U/ml PEG-catalase or 1 μ*M* PKCε inhibitor for 15 min after AngII stimulation. *$p < 0.01$ *versus* controls, **$p < 0.05$ *versus* AngII ($n = 3$–5). 5HD, 5-hydroxydecanoic acid; ESR, electron spin resonance.

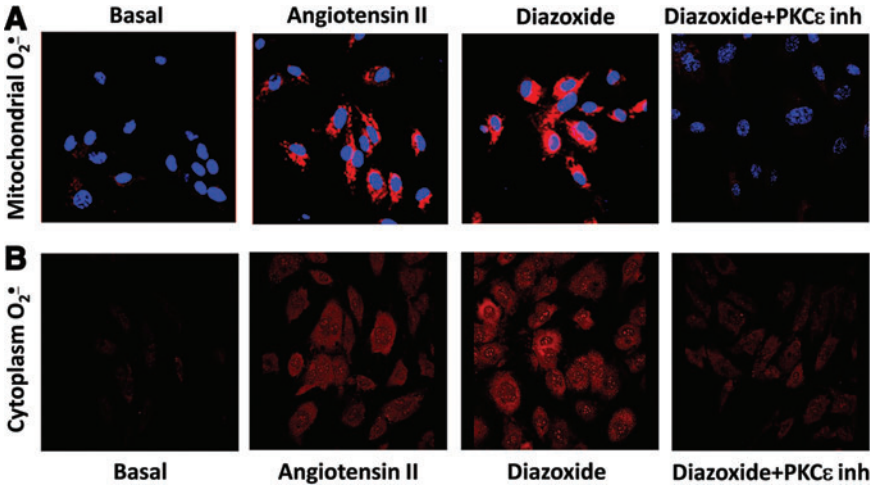

FIG. 8. Stimulation of mitoK$^+_{ATP}$ with diazoxide increases mitochondrial and cytoplasmic $O_2^{\bullet-}$. (A) Mitochondrial $O_2^{\bullet-}$ measured with MitoSOX (2 μM) after the stimulation of HAEC with AngII or diazoxide (100 nM) plus PKCε inhibitor (1 μM). **(B)** Cytoplasm $O_2^{\bullet-}$ measured with DHE (10 μM) in HAEC treated with AngII (200 nM, 4 h) or diazoxide (100 nM, 10 min) plus PKCε inhibitor (1 μM). Figure show typical images from confocal microscopy studies obtained in five independent experiments. To see this illustration in color, the reader is referred to the web version of this article at www.liebertpub.com/ars

MitoSOX fluorescence (Fig. 8A). This increase was similar to that observed in AngII-stimulated cells. This effect of diazoxide was abolished by the inhibition of PKCε emphasizing that PKCε is upstream of mitoK$_{ATP}$. Interestingly, diazoxide also increased $O_2^{\bullet-}$ production in the cytoplasm (Fig. 8B) as evident by an increase of DHE fluorescence. Diazoxide increased cytoplasmic $O_2^{\bullet-}$ to a similar extent as AngII, and this effect was also blocked by PKCε peptide antagonist.

These data confirmed feed-forward regulation of cytoplasmic $O_2^{\bullet-}$ by mitochondrial ROS; however, the exact molecular mechanisms remain elusive. Mitochondrial H_2O_2 is freely diffusible and can stimulate the extramitochondrial NADPH oxidase *via* c-Src-mediated mechanisms (50). We therefore tested the hypothesis that mitochondrial ROS can activate c-Src and that mitochondria targeted antioxidants would attenuate c-Src activation. The activity of c-Src was measured by autocatalytic c-Src phosphorylation. Acute treatment with AngII and bolus addition of H_2O_2 (200 μM) sharply stimulated c-Src phosphorylation (Fig. 9A). Interestingly, acute addition of diazoxide and 4 h treatment increased the c-Src activity to a similar extent as in AngII-stimulated cells. Acute mitoTEMPO treatment with after 4 h stimulation with AngII significantly inhibited the c-Src activity (p-c-Src/c-Src ratio 55% ± 6% *vs.* AngII 4 h), but pretreatment of HAEC

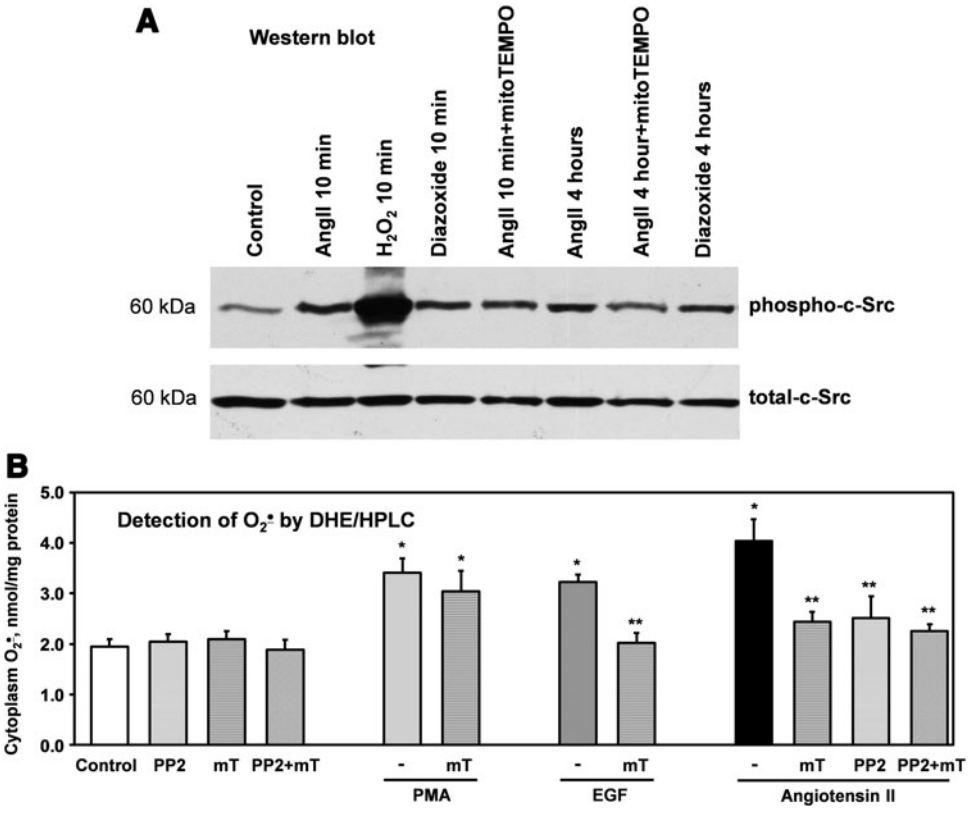

FIG. 9. Inhibition of c-Src activity and cytoplasmic $O_2^{\bullet-}$ by mitochondria targeted SOD mimetic mitoTEMPO in AngII or EGF-stimulated HAEC. (A) Western blot analysis of active phosphorylated c-Src was measured in HAEC treated with diazoxide or AngII for 10 min or 4 h. Some samples were incubated with mitoTEMPO (25 nM) for 15 min before collection of cells for Western blot analysis. Figure show representative Western blot of total c-Src and phosphorylated c-Src obtained in three independent experiments as described previously (6). **(B)** Analysis of cytoplasmic $O_2^{\bullet-}$ production in HAEC stimulated with PMA, EGF, or AngII in the presence of c-Src inhibitor PP2 (10 μM) or mitoTEMPO (mT, 25 nM). *$p < 0.01$ *versus* control, **$p < 0.05$ *versus* AngII ($n = 3$–5). PMA, phorbol myristate acetate; SOD, superoxide dismutase.

with mitoTEMPO prior 10 min AngII stimulation did not significantly affect the c-Src activity (p-c-Src/c-Src ratio 91% ± 7% *vs*. AngII 10 min). This can be explained by the presence of two phases of c-Src activation (45). Acute c-Src activation is not redox sensitive and depends on AT1 receptor activation. The second phase during long-term AngII stimulation is redox dependent (45) and in our experiment was attenuated by mitoTEMPO.

c-Src is an important modulator of NADPH oxidase activity. We therefore investigated the functional role of c-Src regulation by mitochondrial ROS by measuring c-Src-dependent production of cytoplasmic $O_2^{\bullet -}$ in the absence or presence of mitoTEMPO. Four-hour stimulation of HAEC with AngII significantly increased cytoplasmic $O_2^{\bullet -}$ measured by HPLC and DHE (Fig. 9B). Both acute treatment with the c-Src inhibitor PP2 and mitoTEMPO supplementation attenuated $O_2^{\bullet -}$ production caused by AngII. The combination of PP2 and mitoTEMPO did not further decrease $O_2^{\bullet -}$, supporting the action of PP2 and mitoTEMPO on the same pathway of NADPH oxidase activation.

To verify the c-Src-dependent activation of NADPH oxidases by mitochondrial ROS, we compared the effect of mitoTEMPO on phorbol myristate acetate (PMA)- and EGF-induced production of cytoplasmic $O_2^{\bullet -}$. PMA activates NADPH oxidase *via* a PKC-dependent pathway, whereas EGF stimulates NADPH oxidase through c-Src. MitoTEMPO inhibited the EGF stimulated $O_2^{\bullet -}$ but did not affect PMA-stimulated activation (Fig. 9B). These data, therefore, support the role of c-Scr in the activation of NADPH oxidases by mitochondrial ROS.

Inhibition of AngII-induced $O_2^{\bullet -}$ and hypertension by scavenging of mitochondrial H_2O_2

To test the role of mitochondrial H_2O_2 in the stimulation of AngII-induced $O_2^{\bullet -}$ and its contribution in hypertension, we used mitochondria-targeted glutathione peroxidase mimetic mitoEbselen, also known as MitoPeroxidase (46). It was found that acute treatment of AngII-stimulated HAEC with mitoEbslen (1 n*M*) inhibited the production of cytoplasmic $O_2^{\bullet -}$, whereas supplementation of untargeted H_2O_2 scavenger ebselen (1 n*M*) did not significantly affect $O_2^{\bullet -}$ production (Fig. 10A). As expected, basal $O_2^{\bullet -}$ production in unstimulated cells was not affected neither by mitoEbselen nor

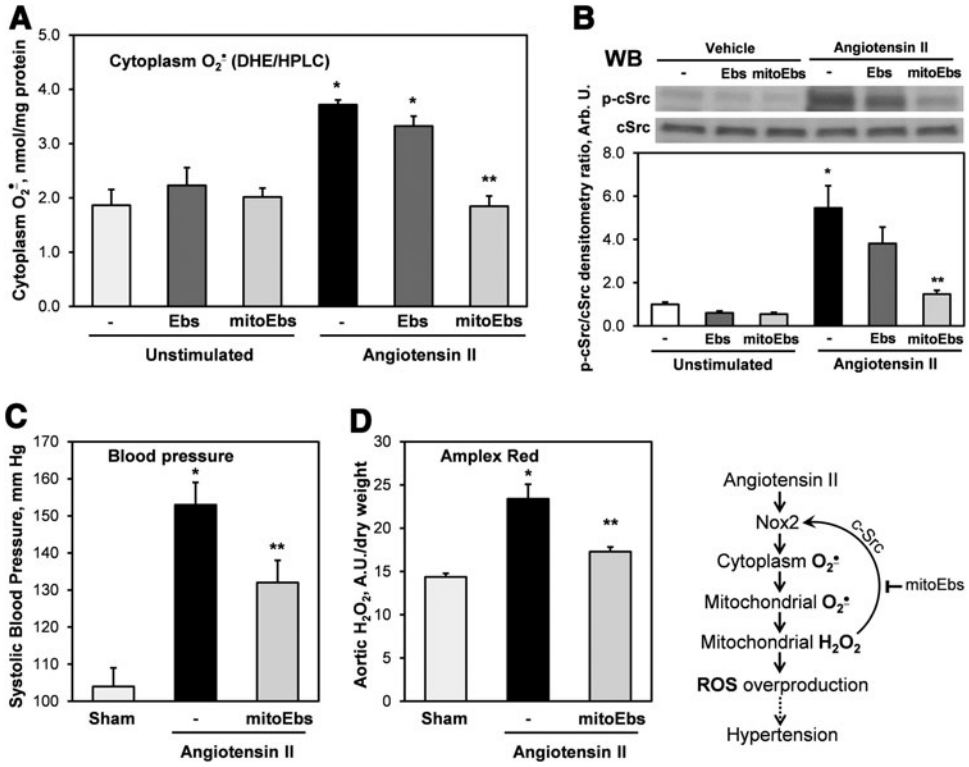

FIG. 10. Inhibition of AngII-induced vascular ROS production and hypertension by mitochondrial H_2O_2 scavenger mitoEbselen. (A) Measurements of cytoplasmic $O_2^{\bullet -}$ in intact HAEC using DHE (10 μM) and HPLC. HAEC were stimulated with AngII (200 n*M*) for 4 h and then supplemented with ebselen (1 n*M*), mitoEbselen (1 n*M*), or DMSO as a vehicle for 15 min before incubation with DHE. Results are mean ± SEM. *$p < 0.01$ *versus* control, **$p < 0.05$ *versus* AngII. **(B)** Western blot analysis of active phosphorylated c-Src was measured in HAEC treated with AngII (200 n*M*) for 4 h. Some samples were incubated with Ebselen (1 n*M*) or mitoEbselen (1 n*M*) for 15 min before the collection of cells for Western blot analysis. Figure shows representative Western blot of total c-Src and phosphorylated c-Src obtained in three independent experiments. Data are presented as densitometry ratio of p-c-Src/c-Src. **(C)** Systolic blood pressure in mice infused for 7 days with saline (control), AngII (0.7 mg/kg/day), and then co-infused for 7 days with mitoEbselen (0.7 mg/kg/day) or DMSO as a vehicle after the onset of AngII-induced hypertension. **(D)** Amplex Red measurements of H_2O_2 in aorta isolated from mice infused with mitoEbslen or DMSO after the onset of AngII-induced hypertension. Results represent mean ± SEM for four to eight animals per group. *$p < 0.01$ *versus* control, **$p < 0.05$ *versus* AngII. ROS, reactive oxygen species.

by ebselen since it is not redox dependent. These data support the role of mitochondrial H_2O_2 in the stimulation of AngII-induced cytoplasmic $O_2^{\bullet -}$ in endothelial cells.

Our data indicate that c-Src inhibition and blocking of mitochondrial H_2O_2 attenuated $O_2^{\bullet -}$ production to similar level of unstimulated cells (Figs. 7B and 8A), which suggest that c-Src is stimulated by mitochondrial H_2O_2. We have directly tested this hypothesis by the analysis of c-Src phosphorylation in AngII-stimulated cells following treatment with DMSO (vehicle), ebselen, or mitoEbslen. Indeed, acute treatment of AngII-stimulated cells by mitoEbselen (1 n*M*) inhibited c-Src activity almost to the basal level, whereas untargeted ebselen (1 n*M*) did not have significant effect (Fig. 10B). These data support the role of mitochondrial H_2O_2 in the stimulation of c-Src-dependent NADPH oxidase in AngII-stimulated endothelial cells.

The pathophysiological role of mitochondrial H_2O_2 in hypertension was investigated in mice treated with mitoEbselen after the onset of AngII-induced hypertension. Following 6 days of AngII infusion, mice were treated with mitoEbselen (0.7 mg/kg/day) or DMSO as a vehicle using osmotic minipump. Treatment of hypertensive mice with mitoEbselen significantly reduced blood pressure (Fig. 10C). Reduction of vascular H_2O_2 was confirmed by the analysis of H_2O_2 in intact aorta using Amplex Red assay. It was found that AngII infusion significantly increased aortic H_2O_2 production but mitoEbselen treatment substantially reduced H_2O_2 level (Fig. 10D). These data support the role of mitochondrial H_2O_2 in the stimulation of c-Src-dependent NADPH oxidase and its contribution in hypertension.

Discussion

The present study provides the first evidence that the Nox2 isoform of vascular NADPH oxidase is responsible for AngII-mediated stimulation of mitochondrial ROS in human endothelial cells. We have found that AngII stimulates the production of mitochondrial ROS *via* the activation of reverse electron transfer. Analyses of isolated mitochondria have demonstrated an important role of PKCε in the regulation of mitochondrial ROS. Our data indicate that PKCε activates mitoK$_{ATP}$, which triggers mitochondrial reverse electron transfer (Fig. 9). Interestingly, inhibition of mitochondrial ROS production with malate, malonate, rotenone, PKCε, or 5HD (20) abolished AngII-induced $O_2^{\bullet -}$ production in the cytoplasm. These data imply feed-forward regulation of cytoplasmic NADPH oxidase by mitochondrial ROS. Our experiments with diazoxide confirmed this cross-talk between mitochondrial ROS and NADPH oxidase activity since diazoxide increased the production of mitochondrial $O_2^{\bullet -}$, which led to the stimulation of cytoplasmic c-Src and downstream activation of NADPH oxidase. Finally, the role of mitochondrial reverse electron transfer in AngII-mediated vascular oxidative stress and hypertension was determined in *in vivo* experiments where we showed that malate inhibits endothelial oxidative stress and decreases blood pressure in AngII-infused mice.

We have previously shown that AngII stimulates the production of mitochondrial $O_2^{\bullet -}$ (20). This increase was dependent on NADPH oxidase activity because siRNA-induced depletion of the NADPH oxidase subunit p22^{phox}, or inhibition of NADPH oxidase activity by apocynin, prevented mitochondrial impairment and attenuated the production of mitochondrial $O_2^{\bullet -}$, demonstrating an upstream role of the NADPH oxidase in the activation of mitochondrial $O_2^{\bullet -}$. In the current study, we have investigated the specific NADPH isoform responsible for this AngII-mediated effect on mitochondria. We found that the depletion of Nox2 inhibited AngII-induced production of mitochondrial $O_2^{\bullet -}$ (Fig. 1). It is important to note that Western blots showed that Nox2 is exclusively localized in the cytoplasm and not in the mitochondria (Fig. 2). These data suggest that ROS produced in the cytoplasm by Nox2 signal to redox-dependent targets in the mitochondria. We suggest that an important downstream target is mitochondrial PKCε. Indeed, the inhibition of PKCε in isolated mitochondria completely abolished AngII-induced production of mitochondrial ROS (Fig. 5A). Our data indicate that the activation of redox-sensitive PKCε activates mitoK$_{ATP}$ and that opening of mitoK$_{ATP}$ leads to the activation of reverse electron transfer (Fig. 9). Interestingly, it has been recently shown that superoxide can directly activate mitoK$_{ATP}$ (43), which may explain why overexpression of SOD2 or mitoTEMPO supplementation inhibit the production of mitochondrial ROS (17). This provides an important insight into the molecular mechanisms in the regulation of mitochondrial ROS. We suggest that ROS production by mitochondrial reverse electron transfer is an important physiological function that can be regulated by redox-sensitive PKCε and mitoK$_{ATP}$ (11, 43).

Our data demonstrate redox-dependent stimulation of mitochondrial ROS by Nox2 in endothelial cells. Other cell types, however, have a different pattern of Nox isoform distribution. Vascular smooth muscle cells, for example, express Nox1, which is upregulated by AngII (15), and therefore, Nox1 can play an important role in cross-talk between mitochondrial ROS and NADPH oxidase vascular smooth muscle cells. Indeed, both AngII and diazoxide stimulated mitochondrial ROS and NADPH oxidase in rat vascular smooth muscle cells *in vitro* and in rat aorta (29).

It has been recently reported that Nox4 is present in the mitochondria of rat kidney in podocytes, glomerular mesangial and tubular epithelial cells (7), and in the mitochondria of cardiac myocytes (32). Confocal microscopy showed significant co-localization of Nox4 with mitochondrial F1F0-ATP synthase, as well as p22phox subunit of NADPH oxidases (7). Unfortunately, current methods do not provide measurements of specific Nox4 activity. These studies, therefore, remain controversial due to the lack of specific Nox4 activity data in mitochondrial preparations. Our studies did not show the presence of Nox1, Nox2, Nox4, and p22phox subunits in the mitochondria of endothelial cells and mouse vascular tissue arguing against the mitochondrial localization of NADPH oxidases in these tissues (20). It has been previously shown that Nox4 is localized in focal adhesions, along stress fibers, and in the nucleus (27, 38). It is possible that mitochondrial localization of Nox4 reported by Block *et al.* (7) and Ago *et al.* (2) differ from previous publications (27, 38) due to distinct Nox4 antibodies used for immunostaining. The difference in Nox4 localization could be also due to the fact that these research groups have investigated different cell types and Nox4 localization in mitochondria may be cell-type specific. We and others have previously shown that Nox4 predominantly produces H_2O_2 (15, 47), and it is plausible that Nox4-mediated H_2O_2 production can stimulate

redox-sensitive upregulation of mitochondrial ROS. Recent publication of Kozieł *et al.* have shown that depletion of Nox4 in the late 25th passage of human umbilical vein endothelial cells reduced the production of mitochondrial ROS, increased complex I activity, and improved mitochondrial respiration. These data support redox-dependent regulation of mitochondrial function by Nox4 (21). Although our data indicate the lack of Nox4 in human aortic endothelial mitochondria, it is conceivable that mitochondrial Nox4 localization is cell-, tissue-, and species-specific. For example, Case *et al.* showed that siRNA-mediated knockdown of Nox4 decreased AngII-induced mitochondrial $O_2^{\bullet -}$ production in catecholaminergic neuronal cell, supporting the role of Nox4 in neuronal regulation of mitochondrial ROS (9). Considering the controversy and inconsistent observations, mitochondrial expression of Nox4 and its functional significance require additional studies.

Mitochondrial reverse electron transfer has been previously suggested as a major source of mitochondrial ROS under physiological conditions (42) and that mitochondrial ROS play a key role in cell signaling (54). Indeed, mitochondria regulate intracellular calcium and this is attenuated by the inhibition of $mitoK_{ATP}$ with 5HD (52), which, according to our data, inhibits the production of mitochondrial ROS *via* reverse electron transfer (Figs. 3, 5, and 9). This work provides further insight into the role of mitochondrial ROS in cell signaling. We found that the release of mitochondrial H_2O_2 activates c-Src, which is one of the key mediators of signaling networks (24). Activation of c-Src by mitochondrial ROS may have both physiological and pathological consequences. Interestingly, mitochondrial H_2O_2 contributes to flow-induced dilation in human coronary resistance arteries, which was attenuated by rotenone (37). In our case, blocking mitochondrial reverse electron transfer or treatment with the mitochondria targeted antioxidant mitoTEMPO reduced c-Src activity, decreased NADPH oxidase activity (17), and diminished the production of cellular $O_2^{\bullet -}$ (Figs. 7 and 8). We expect that malate treatment attenuates AngII-induced hypertension by blocking the same c-Src-dependent oxidative stress *in vivo*. Since c-Src has been a pharmacological target for the treatment of cancer and inflammation (40, 49), it is interesting to speculate that mitochondrial ROS and reverse electron transfer may play a role under these pathological conditions.

The data described above suggest that the NADPH oxidases may stimulate the mitochondrial ROS production and vice versa. This represents an ongoing feed-forward cycle, which can be stopped by inhibitors of PKCε, $mitoK_{ATP}$, blocking reverse electron transfer or mitoTEMPO treatment (Fig. 11). Indeed, it has been recently shown that rotenone attenuates DOCA-salt hypertension (53). Rotenone treatment, however, increases oxidative stress in healthy tissue and particularly in the brain, and can lead to the development of Parkinson's disease (41). Inhibition of $mitoK_{ATP}$ in hypertensive conditions (53) is also problematic since this would attenuate important physiological functions of $mitoK_{ATP}$ in heart, vascular and brain tissues. We, therefore, suggest more realistic metabolic targeting of reverse electron transfer with malate. Malate is part of the mitochondrial Krebs cycle and does not have cytotoxic side effects. It is converted into oxaloacetate, which inhibits complex II activity and therefore attenuates the production of mitochondrial $O_2^{\bullet -}$ by reverse electron transfer (42). Application of mitochondria targeted antioxidants such as mitoTEMPO might also be advantageous since mitoTEMPO specifically affects redox activation of $mitoK_{ATP}$ only at the site of enhanced mitochondrial oxidative stress.

Taken together, our data indicate that the interplay between mitochondrial and NADPH oxidase-derived $O_2^{\bullet -}$ constitutes a feed-forward cycle in which Nox2 increases the production of mitochondrial ROS by reverse electron transfer. Enhanced production of mitochondrial ROS further activates the cytoplasmic NADPH oxidases, increasing cellular $O_2^{\bullet -}$ production, diminishing $NO^{\bullet}$ bioavailability, and uncoupling eNOS (8, 17). The effect of ROS on $O_2^{\bullet -}$ production by mitochondria and NADPH oxidase is redox sensitive at the PKCε, $mitoK_{ATP}$, and c-Src sites, which could explain why mitoTEMPO decreased the NADPH oxidase activity and reduced blood pressure in hypertensive animals (17). Our

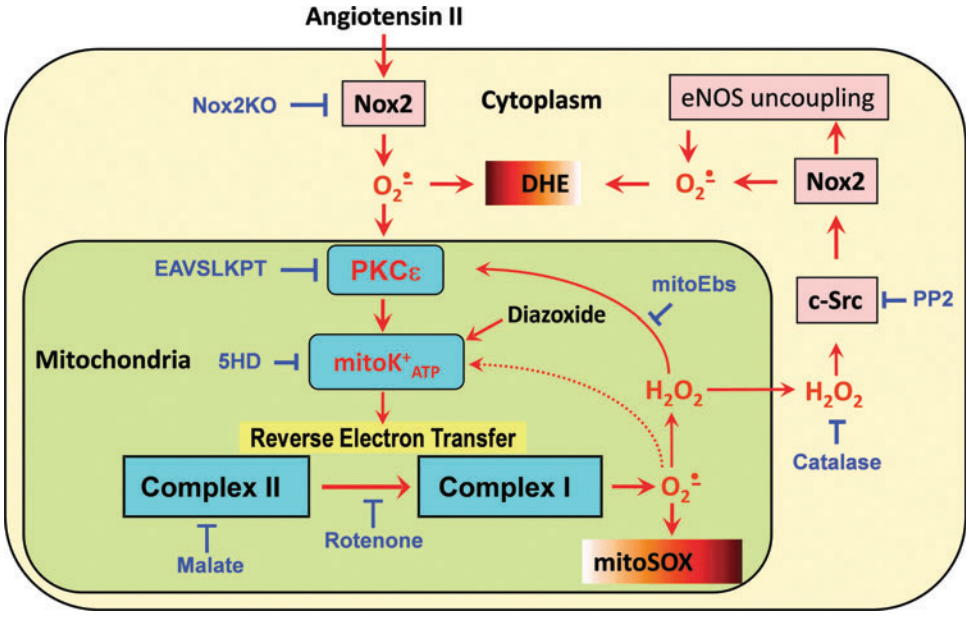

FIG. 11. Nox2 and reverse electron transfer in AngII-induced production of mitochondrial $O_2^{\bullet -}$- and c-Src-dependent feed-forward stimulation of cellular $O_2^{\bullet -}$ production. To see this illustration in color, the reader is referred to the web version of this article at www.liebertpub.com/ars

current findings indicate that scavenging of mitochondrial $O_2^{\bullet-}$ using mitochondria-targeted antioxidants or inhibition of reverse electron transfer can interrupt this vicious cycle and downregulate NADPH oxidase activity (Fig. 11) (17). The interplay between mitochondrial ROS and NADPH oxidases demonstrated here in endothelial cells is likely to be found in other cells and tissues in various pathological conditions associated with AngII, high glucose, fat, or hypoxia and could contribute to the development of many pathological conditions (13). Our study, therefore, shows that Nox2 and mitochondrial reverse electron transfer can be important targets for the development of antioxidant strategies.

Materials and Methods

Reagents

DHE (M-36008) and MitoSOX (D-1168) were supplied by Invitrogen. NADPH oxidase antibodies were obtained from Abcam. PKCε peptide antagonist EAVSLKPT and c-Src antibodies were received from Millipore Corporation. Mito-TEMPO and mitoEbselen were purchased from Enzo Life Sciences. The Nox2 inhibitor peptide gp91ds (CSTRIRRQL) was purchased from GenScript. Rabbit polyclonal Akt antibodies and mouse monoclonal cytochrome *c* antibodies were obtained from Cell Signaling and Santa Cruz Biotechnology. All other reagents were obtained from Sigma.

Cell culture

Human aortic endothelial cells (HAEC) were purchased from Lonza and cultured in EGM-2 medium supplemented with 2% FBS but without antibiotics. On the day before the study, the FBS concentration was reduced to 1%. In preliminary experiments, we examined the effect of varying doses of AngII on cellular $O_2^{\bullet-}$ production. We found that 4 h of AngII increased cellular $O_2^{\bullet-}$ in a dose-dependent manner with maximum stimulation at 200 n*M* (17). This concentration was therefore used in the remainder of the experiments. It should be noted that due to degradation in culture, the steady-state concentration of AngII is substantially lower than that initially added (28).

Nox depletion

To deplete protein levels of the catalytic subunits of NADPH oxidase, we inhibited the expression of Nox1, Nox2, Nox4, and Nox5 using siRNA from Applied Biosystems Ambion. As a control, we used NS siRNA (Applied Biosystems Ambion). The annealed siRNA duplexes for Nox1 (sense, 5′-CAUCCAGCUGUACCUCAGU-3′; antisense 5′-GACCAUCCACUUCAAUCCU-3′), Nox2 (sense 5′-CGUC UUCCUCUUUGUCUGG-3′; antisense 5′-CCAGACAAAGA GGAAGACG-3′), Nox4 (sense, 5′-ACUGAGGUACAGCU GGAUGUU-3′; antisense 5′-CAUCCAGCUGUACCUCAGU UU-3′), and Nox5 (sense 5′-GGUGGACUUUAUCUGGAUC-3′; antisense 5′-GAUCCAGAUAAAGUCCACC-3′).

Expression of catalytic subunits of NADPH oxidase was studied by Western blot analysis (Supplementary Fig. S1) using previously characterized rabbit polyclonal antibodies at 1:1000 dilution (15, 26). Nox1 antibodies were provided by Santa Cruz. Nox2 antibodies were purchased from Millipore. Nox4 and Nox5 antibodies were received from Abcam.

Mitochondrial isolation and study

Mitochondria were isolated as previously described (48). Mitochondrial H_2O_2 was measured by mixing 20 μg of mitochondrial protein with horseradish peroxidase (HRP) (2 U/ml), peroxidase substrate acetamidophenol (1 m*M*), SOD (50 U/ml), and spin probe CAT1H (1 m*M*) in the presence of complex II substrate succinate (20). Production of mitochondrial $O_2^{\bullet-}$ was visualized in intact cultured HAEC using the fluorescent probe MitoSOX (Ex/Em: 510/580 nm; Invitrogen) (12). HAEC were incubated with 2 μ*M* MitoSOX in Kreb-Hepes buffer (KHB) for 20 min at 37°C in a CO_2 incubator. The mitochondrial subcellular location of MitoSOX was confirmed by co-labeling with 50 n*M* MitoTracker Green FM (Ex/Em: 490/516 nm) (17).

Animal experiments

Hypertension was induced by AngII (490 ng/kg/min) as described previously (16) using C57Bl/6J or gp91phoxKO mice (Jackson Labs). In addition, 6 days after saline or AngII minipump placement, mice received a second minipump for infusion of saline as vehicle, malate, mitoTEMPO, or malate plus mitoTEMPO as described in the figure legends. To test the role of mitochondrial H_2O_2, mice received a second minipump with of 50% DMSO as vehicle or mitochondria-targeted H_2O_2 scavenger mitoEbselen. Blood pressure was monitored by the tail cuff method as previously described (31, 51).

Superoxide measurements using HPLC

Cells were cultured up to 80% confluence. Stock solutions of MitoSOX (4 m*M*) and DHE (10 m*M*) in DMSO were prepared and were diluted in KHB to a final concentration of 2 μ*M* MitoSOX and 10 μ*M* DHE. Cells loaded with dye were incubated in a tissue culture incubator for 20 min. Next, buffer was aspirated and scraped cells were mixed with methanol (300 μl) and homogenized with a glass pestle. The cell homogenate was passed through a 0.22-μm syringe filter and methanol filtrates were analyzed by HPLC according to previously published protocols (14). DHE and MitoSOX oxidation products, 2-hydroxyethidium and ethidium, were separated using a C-18 reverse-phase column (Nucleosil 250 to 4.5 mm) and a mobile phase containing 0.1% trifluoroacetic acid and an acetonitrile gradient (from 37% to 47%) at a flow rate of 0.5 ml/min. Ethidium and 2-hydroxyethidium were detected with a fluorescence detector using an emission wavelength of 580 nm and an excitation of 480 nm. Production of cytoplasmic and mitochondrial $O_2^{\bullet-}$ was measured as accumulation of 2-hydroxyethidium and mito-2-hydroxyethidium in DHE or mitSOX supplemented samples as described previously (17).

Confocal microscopy

Intact cells cultured on coverslips were incubated with a fluorescent probe in KHB for 20 min at 37°C in a CO_2 incubator. Production of mitochondrial $O_2^{\bullet-}$ was visualized using the 2 μ*M* fluorescent probe MitoSOX (Ex/Em 405/480 nm). For detection of cytoplasmic $O_2^{\bullet-}$, cells were stained with 10 μ*M* DHE (Ex 405/480 nm). Mitochondria localization was ensured by mitoTracker Green (Ex 488/520 nm). Nuclei were stained with DAPI (Ex 364/461). Mitochondrial

membrane potential was monitored with fluorescent probe TMRM (543/573 nm). Paraformaldehyde fixed cells were mounted in Vectashield (Vector Laboratories) and examined in a confocal imaging system (Zeiss LSM 510 META). For double-labeling experiments, images were scanned with the multitracking mode on a Zeiss LSM 510 META confocal microscope. To distinguish random color overlap from co-localization, Imaris Coloc software was used.

We have previously showed co-localization of MitoSOX staining with specific mitoTracker, and MitoSOX-$O_2^{\bullet -}$-specific HPLC signal was stimulated by the treatment of endothelial cells with antimycin A and inhibited by mitoTEMPO (17). Meanwhile, DHE-$O_2^{\bullet -}$-specific HPLC signal was stimulated by PMA and inhibited after Nox2 depletion but was not affected by antimycin A (17). MitoSOX, therefore, provides mitochondria-specific $O_2^{\bullet -}$ measurements, whereas DHE does not detect mitochondrial $O_2^{\bullet -}$ since it is not sensitive to antimycin A. Cellular DHE signal mainly reflects $O_2^{\bullet -}$ production in the cytoplasm and the lumen of intracellular organelles. In this article, we used MitoSOX for mitochondria-specific $O_2^{\bullet -}$ detection while DHE fluorescence was identified as cytoplasm $O_2^{\bullet -}$ due to its diffuse intracellular localization.

In this study, we used lower MitoSOX concentration, which may explain discrepancy in the images compared with the previous publication. Rotenone can induce ROS production on complex I since it overreduces ubiquinone domain (41). ROS stimulation by rotenone was observed only in non-stimulated cells, whereas supplementation of rotenone after AngII treatment actually inhibits AngII-induced $O_2^{\bullet -}$ production. This paradoxical rotenone effect is due to the inhibition of reverse electron transfer in AngII-treated cells, which was absent in the nonstimulated cells (Figs. 3 and 4).

Electron spin resonance measurement of mitochondrial H_2O_2 production. Mitochondrial H_2O_2 was measured by HRP-mediated oxidation of spin probe CAT1H as described previously (19). This method takes advantage of the electron spin resonance (ESR), which provides high sensitivity ROS measurements in nontransparent samples such as mitochondrial suspension or cellular homogenates with detection limit as low as 1 pmol/mg protein/min using only 20 μg protein. Mitochondria were incubated with 10 m*M* succinate in the presence of 1 m*M* 4-acetamidophenol, 2 U/ml HRP, 50 U/ml Cu/Zn-SOD, and 1 m*M* CAT1H in media containing 125 m*M* KCl, 10 m*M* MOPS, 2 m*M* $MgSO_4$, 2 m*M* KH_2PO_4, 10 m*M* NaCl, 1 m*M* EGTA, and 0.7 m*M* $CaCl_2$, pH 7.2. This method is based on reaction of HRP with H_2O_2 generating HRP compound I, which in turn oxidizes 4-acetamidophenol. Subsequently, 4-acetamidophenol radical oxidizes CAT1H to its corresponding stable nitroxide CAT1, which is quantitatively detected by ESR. Specificity of H_2O_2 detection was confirmed by inhibiting the ESR signal with 50 μg/ml catalase.

ESR Experiments. All ESR samples were placed in 50-μl glass capillaries (Corning). ESR spectra were recorded using an EMX ESR spectrometer (Bruker Biospin Corp.) and a super high Q microwave cavity at room temperature. The ESR settings for field-scan experiments with the spin probe CAT1H were as follows: field sweep, 70 Gauss; microwave frequency, 9.82 GHz; microwave power, 20 milliwatts; modulation amplitude, 0.7 Gauss; conversion time, 41 ms; time constant, 164 ms; and receiver gain, 1×10^5 ($n=4$ scans). The rates of H_2O_2 production were determined by monitoring the amplitude of the low-field component of the ESR spectrum of CAT1-nitroxide with the following settings: field sweep, 60 Gauss; microwave frequency, 9.46 GHz; microwave power, 20 milliwatts; modulation amplitude, 2 Gauss; conversion time, 1311 ms; time constant, 5243 ms; and receiver gain, 1×10^5. ESR experiments were repeated at least three times.

Statistics

Experiments were analyzed using the Student Neuman Keuls *post-hoc* test and analysis of variance. p levels < 0.05 were considered significant.

Acknowledgments

We are grateful to Dr. Igor A. Kirilyuk and Dr. Igor. A. Grigor'ev for their assistance with mitochondria-targeted antioxidants and thank Dr. Alexander Panov and Dr. Vladimir Mayorov for their fruitful discussion and technical assistance.

Sources of Funding

This work was supported by funding from National Institutes of Health grant HL094469, HL093115 and American Heart Association Grant-in-Aid 09GRNT2220128.

Author Disclosure Statement

The authors have no conflicts of interest to disclose.

References

1. Ago T, Kitazono T, Ooboshi H, Iyama T, Han YH, Takada J, Wakisaka M, Ibayashi S, Utsumi H, and Iida M. Nox4 as the major catalytic component of an endothelial NAD(P)H oxidase. *Circulation* 109: 227–233, 2004.
2. Ago T, Kuroda J, Pain J, Fu C, Li H, and Sadoshima J. Upregulation of Nox4 by hypertrophic stimuli promotes apoptosis and mitochondrial dysfunction in cardiac myocytes. *Circ Res* 106: 1253–1264, 2010.
3. Andrukhiv A, Costa AD, West IC, and Garlid KD. Opening mitoKATP increases superoxide generation from complex I of the electron transport chain. *Am J Physiol Heart Circ Physiol* 291: H2067–H2074, 2006.
4. Beckman JS, Minor RL, Jr., White CW, Repine JE, Rosen GM, and Freeman BA. Superoxide dismutase and catalase conjugated to polyethylene glycol increases endothelial enzyme activity and oxidant resistance. *J Biol Chem* 263: 6884–6892, 1988.
5. Bendall JK, Rinze R, Adlam D, Tatham AL, de Bono J, Wilson N, Volpi E, and Channon KM. Endothelial Nox2 overexpression potentiates vascular oxidative stress and hemodynamic response to angiotensin II: studies in endothelial-targeted Nox2 transgenic mice. *Circ Res* 100: 1016–1025, 2007.
6. Block K, Eid A, Griendling KK, Lee DY, Wittrant Y, and Gorin Y. Nox4 NAD(P)H oxidase mediates Src-dependent tyrosine phosphorylation of PDK-1 in response to angiotensin II: role in mesangial cell hypertrophy and fibronectin expression. *J Biol Chem* 283: 24061–24076, 2008.
7. Block K, Gorin Y, and Abboud HE. Subcellular localization of Nox4 and regulation in diabetes. *Proc Natl Acad Sci U S A* 106: 14385–14390, 2009.
8. Boulden BM, Widder JD, Allen JC, Smith DA, Al-Baldawi RN, Harrison DG, Dikalov SI, Jo H, and Dudley SC, Jr. Early

determinants of H2O2-induced endothelial dysfunction. *Free Radic Biol Med* 41: 810–817, 2006.
9. Case AJ, Li S, Basu U, Tian J, and Zimmerman MC. Mitochondrial-localized NADPH oxidase 4 is a source of superoxide in angiotensin II-stimulated neurons. *Am J Physiol Heart Circ Physiol* 305: H19–H28, 2013.
10. Chobanian AV, Bakris GL, Black HR, Cushman WC, Green LA, Izzo JL, Jr., Jones DW, Materson BJ, Oparil S, Wright JT, Jr., and Roccella EJ. Seventh report of the joint national committee on prevention, detection, evaluation, and treatment of high blood pressure. *Hypertension* 42: 1206–1252, 2003.
11. Costa AD and Garlid KD. Intramitochondrial signaling: interactions among mitoKATP, PKCepsilon, ROS, and MPT. *Am J Physiol Heart Circ Physiol* 295: H874–H882, 2008.
12. Csiszar A, Labinskyy N, Zhao X, Hu F, Serpillon S, Huang Z, Ballabh P, Levy RJ, Hintze TH, Wolin MS, Austad SN, Podlutsky A, and Ungvari Z. Vascular superoxide and hydrogen peroxide production and oxidative stress resistance in two closely related rodent species with disparate longevity. *Aging Cell* 6: 783–797, 2007.
13. Dikalov S. Cross talk between mitochondria and NADPH oxidases. *Free Radic Biol Med* 51: 1289–1301, 2011.
14. Dikalov S, Griendling KK, and Harrison DG. Measurement of reactive oxygen species in cardiovascular studies. *Hypertension* 49: 717–727, 2007.
15. Dikalov SI, Dikalova AE, Bikineyeva AT, Schmidt HH, Harrison DG, and Griendling KK. Distinct roles of Nox1 and Nox4 in basal and angiotensin II-stimulated superoxide and hydrogen peroxide production. *Free Radic Biol Med* 45: 1340–1351, 2008.
16. Dikalova A, Clempus R, Lassegue B, Cheng G, McCoy J, Dikalov S, San Martin A, Lyle A, Weber DS, Weiss D, Taylor WR, Schmidt HH, Owens GK, Lambeth JD, and Griendling KK. Nox1 overexpression potentiates angiotensin II-induced hypertension and vascular smooth muscle hypertrophy in transgenic mice. *Circulation* 112: 2668–2676, 2005.
17. Dikalova AE, Bikineyeva AT, Budzyn K, Nazarewicz RR, McCann L, Lewis W, Harrison DG, and Dikalov SI. Therapeutic targeting of mitochondrial superoxide in hypertension. *Circ Res* 107: 106–116, 2010.
18. Dikalova AE, Gongora MC, Harrison DG, Lambeth JD, Dikalov S, and Griendling KK. Upregulation of Nox1 in vascular smooth muscle leads to impaired endothelium-dependent relaxation via eNOS uncoupling. *Am J Physiol Heart Circ Physiol* 299: H673–H679, 2010.
19. Doughan AK and Dikalov SI. Mitochondrial redox cycling of mitoquinone leads to superoxide production and cellular apoptosis. *Antioxid Redox Signal* 9: 1825–1836, 2007.
20. Doughan AK, Harrison DG, and Dikalov SI. Molecular Mechanisms of angiotensin II-mediated mitochondrial dysfunction. linking mitochondrial oxidative damage and vascular endothelial dysfunction. *Circ Res* 102: 488–496, 2008.
21. Koziel R, Pircher H, Kratochwil M, Lener B, Hermann M, Dencher NA, Jansen-Durr P. Mitochondrial respiratory chain complex I is inactivated by NADPH oxidase Nox4. Biochem J 452: 231–239, 2013.
22. Fujii A, Nakano D, Katsuragi M, Ohkita M, Takaoka M, Ohno Y, and Matsumura Y. Role of gp91phox-containing NADPH oxidase in the deoxycorticosterone acetate-salt-induced hypertension. *Eur J Pharmacol* 552: 131–134, 2006.
23. Garlid KD, Paucek P, Yarov-Yarovoy V, Sun X, and Schindler PA. The mitochondrial KATP channel as a receptor for potassium channel openers. *J Biol Chem* 271: 8796–8799, 1996.
24. Griendling KK, Sorescu D, Lassegue B, and Ushio-Fukai M. Modulation of protein kinase activity and gene expression by reactive oxygen species and their role in vascular physiology and pathophysiology. *Arterioscler Thromb Vasc Biol* 20: 2175–2183, 2000.
25. Griendling KK, Sorescu D, and Ushio-Fukai M. NAD(P)H oxidase: role in cardiovascular biology and disease. *Circ Res* 86: 494–501, 2000.
26. Guzik TJ, Chen W, Gongora MC, Guzik B, Lob HE, Mangalat D, Hoch N, Dikalov S, Rudzinski P, Kapelak B, Sadowski J, and Harrison DG. Calcium-dependent NOX5 NADPH oxidase contributes to vascular oxidative stress in human coronar artery disease. *J Am Coll Cardiol* 52: 1803–1809, 2008.
27. Hilenski LL, Clempus RE, Quinn MT, Lambeth JD, and Griendling KK. Distinct subcellular localizations of Nox1 and Nox4 in vascular smooth muscle cells. *Arterioscler Thromb Vasc Biol* 24: 677–683, 2004.
28. Hoch NE, Guzik TJ, Chen W, Deans T, Maalouf SA, Gratze P, Weyand C, and Harrison DG. Regulation of T-cell function by endogenously produced angiotensin II. *Am J Physiol Regul Integr Comp Physiol* 296: R208–R216, 2009.
29. Kimura S, Zhang GX, Nishiyama A, Shokoji T, Yao L, Fan YY, Rahman M, and Abe Y. Mitochondria-derived reactive oxygen species and vascular MAP kinases: comparison of angiotensin II and diazoxide. *Hypertension* 45: 438–444, 2005.
30. Kolosova NG, Akulov AE, Stefanova NA, Moshkin MP, Savelov AA, Koptyug IV, Panov AV, and Vavilin VA. Effect of malate on the development of rotenone-induced brain changes in Wistar and OXYS rats: an MRI study. *Dokl Biol Sci* 437: 72–75, 2011.
31. Krege JH, Hodgin JB, Hagaman JR, and Smithies O. A noninvasive computerized tail-cuff system for measuring blood pressure in mice. *Hypertension* 25: 1111–1115, 1995.
32. Kuroda J, Ago T, Matsushima S, Zhai P, Schneider MD, and Sadoshima J. NADPH oxidase 4 (Nox4) is a major source of oxidative stress in the failing heart. *Proc Natl Acad Sci U S A* 107: 15565–15570, 2010.
33. Lassegue B and Clempus RE. Vascular NAD(P)H oxidases: specific features, expression, and regulation. *Am J Physiol Regul Integr Comp Physiol* 285: R277–R297, 2003.
34. Lassegue B and Griendling KK. NADPH oxidases: functions and pathologies in the vasculature. *Arterioscler Thromb Vasc Biol* 30: 653–661, 2010.
35. Lassegue B, Sorescu D, Szocs K, Yin Q, Akers M, Zhang Y, Grant SL, Lambeth JD, and Griendling KK. Novel gp91(phox) homologues in vascular smooth muscle cells: nox1 mediates angiotensin II-induced superoxide formation and redox-sensitive signaling pathways. *Circ Res* 88: 888–894, 2001.
36. Lavoie JL and Sigmund CD. Minireview: overview of the renin-angiotensin system—an endocrine and paracrine system. *Endocrinology* 144: 2179–2183, 2003.
37. Liu Y, Zhao H, Li H, Kalyanaraman B, Nicolosi AC, and Gutterman DD. Mitochondrial sources of H2O2 generation play a key role in flow-mediated dilation in human coronary resistance arteries. *Circ Res* 93: 573–580, 2003.
38. Lyle AN, Deshpande NN, Taniyama Y, Seidel-Rogol B, Pounkova L, Du P, Papaharalambus C, Lassegue B, and Griendling KK. Poldip2, a novel regulator of Nox4 and cytoskeletal integrity in vascular smooth muscle cells. *Circ Res* 105: 249–259, 2009.
39. Martyn KD, Frederick LM, von Loehneysen K, Dinauer MC, and Knaus UG. Functional analysis of Nox4 reveals unique characteristics compared to other NADPH oxidases. *Cell Signal* 18: 69–82, 2006.

40. Page TH, Smolinska M, Gillespie J, Urbaniak AM, and Foxwell BM. Tyrosine kinases and inflammatory signalling. *Curr Mol Med* 9: 69–85, 2009.
41. Panov A, Dikalov S, Shalbuyeva N, Taylor G, Sherer T, and Greenamyre JT. Rotenone model of Parkinson disease: multiple brain mitochondria dysfunctions after short term systemic rotenone intoxication. *J Biol Chem* 280: 42026–42035, 2005.
42. Panov A, Schonfeld P, Dikalov S, Hemendinger R, Bonkovsky HL, and Brooks BR. The neuromediator glutamate, through specific substrate interactions, enhances mitochondrial ATP production and reactive oxygen species generation in nonsynaptic brain mitochondria. *J Biol Chem* 284: 14448–14456, 2009.
43. Queliconi BB, Wojtovich AP, Nadtochiy SM, Kowaltowski AJ, and Brookes PS. Redox regulation of the mitochondrial K(ATP) channel in cardioprotection. *Biochim Biophys Acta* 1813: 1309–1315, 2011.
44. Selivanov VA, Votyakova TV, Pivtoraiko VN, Zeak J, Sukhomlin T, Trucco M, Roca J, and Cascante M. Reactive oxygen species production by forward and reverse electron fluxes in the mitochondrial respiratory chain. *PLoS Comput Biol* 7: e1001115, 2011.
45. Seshiah PN, Weber DS, Rocic P, Valppu L, Taniyama Y, and Griendling KK. Angiotensin II stimulation of NAD(P)H oxidase activity: upstream mediators. *Circ Res* 91: 406–413, 2002.
46. Smith RA, Hartley RC, and Murphy MP. Mitochondria-targeted small molecule therapeutics and probes. *Antioxid Redox Signal* 15: 3021–3038, 2011.
47. Takac I, Schroder K, Zhang L, Lardy B, Anilkumar N, Lambeth JD, Shah AM, Morel F, and Brandes RP. The E-loop is involved in hydrogen peroxide formation by the NADPH oxidase Nox4. *J Biol Chem* 286: 13304–13313, 2011.
48. Trounce IA, Kim YL, Jun AS, and Wallace DC. Assessment of mitochondrial oxidative phosphorylation in patient muscle biopsies, lymphoblasts, and transmitochondrial cell lines. *Methods Enzymol* 264: 484–509, 1996.
49. Tsygankov AY and Shore SK. Src: regulation, role in human carcinogenesis and pharmacological inhibitors. *Curr Pharm Des* 10: 1745–1756, 2004.
50. Ushio-Fukai M, Griendling KK, Becker PL, Hilenski L, Halleran S, and Alexander RW. Epidermal growth factor receptor transactivation by angiotensin II requires reactive oxygen species in vascular smooth muscle cells. *Arterioscler Thromb Vasc Biol* 21: 489–495, 2001.
51. Widder JD, Guzik TJ, Mueller CF, Clempus RE, Schmidt HH, Dikalov SI, Griendling KK, Jones DP, and Harrison DG. Role of the multidrug resistance protein-1 in hypertension and vascular dysfunction caused by angiotensin II. *Arterioscler Thromb Vasc Biol* 27: 762–768, 2007.
52. Xi Q, Cheranov SY, and Jaggar JH. Mitochondria-derived reactive oxygen species dilate cerebral arteries by activating Ca2+ sparks. *Circ Res* 97: 354–362, 2005.
53. Zhang A, Jia Z, Wang N, Tidwell TJ, and Yang T. Relative contributions of mitochondria and NADPH oxidase to deoxycorticosterone acetate-salt hypertension in mice. *Kidney Int* 80: 51–60, 2011.
54. Zhang DX and Gutterman DD. Mitochondrial reactive oxygen species-mediated signaling in endothelial cells. *Am J Physiol Heart Circ Physiol* 292: H2023–H2031, 2007.

Address correspondence to:
Dr. Rafal R. Nazarewicz
Free Radicals in Medicine Core
Division of Clinical Pharmacology
Vanderbilt University Medical Center
2200 Pierce Ave., 536 RRB
Nashville, TN 37232-6602

E-mail: r.nazar@vanderbilt.edu

Date of first submission to ARS Central, August 26, 2012; date of final revised submission, September 1, 2013; date of acceptance, September 22, 2013.

Abbreviations Used

5HD = 5-hydroxydecanoic acid
AngII = angiotensin II
DHE = dihydroethidium
ESR = electron spin resonance
HAEC = human aortic endothelial cells
HRP = horseradish peroxidase
KHB = Kreb-Hepes buffer
mitoK$^+_{ATP}$ = mitochondrial ATP-sensitive potassium channel
MitoSOX = dihydroethidium conjugate with hexyl triphenylphosphonium
mitoTEMPO = (2-(2,2,6,6-tetramethylpiperidin-1-oxyl-4-ylamino)-2-oxoethyl) triphenylphosphonium
NS siRNA = nonsilencing siRNA
PMA = phorbol myristate acetate
RET = reverse electron transport
ROS = reactive oxygen species
SOD = superoxide dismutase